Ronny Fritzsche, Tobias Rüffer, Heinrich Lang and Michael Mehring*

Synthesis and characterization of $GeH_2Cp^*_2$ and its structural comparison with $SiXHCp^*_2$(X=Cl, H) and $SnCl_2Cp^*_2$

DOI 10.1515/mgmc-2017-0014
Received March 17, 2017; accepted April 10, 2017

Abstract: The organogermane $GeH_2Cp^*_2$ (**1**) was synthesized by the reaction of $GeCl_2Cp^*_2$ (**A**) with $LiAlH_4$ in quantitative yield, whereas the synthesis of the previously reported compounds $SiCl_2Cp^*_2$ (**B**), $SnCl_2Cp^*_2$ (**C**), $SiClHCp^*_2$ (**D**) and $SiH_2Cp^*_2$ (**E**) followed established routes. The molecular structures of the Cp*M(IV) derivatives **1**, **B**, **D** and **E** are reported. In addition, compound **1** was characterized by spectroscopic methods such as ^1H and $^{13}C\{^1H\}$ NMR spectroscopy, ATR-FTIR spectroscopy and EI-mass spectrometry. The thermal behavior of the germanes **1** and **A** was investigated by thermogravimetric analysis (TGA, DSC) and PXRD. The decomposition of compounds **A** and **1** starts at 270°C (**A**) and 200°C (**1**), respectively. The formation of crystalline Ge upon heating these compounds in sealed quartz glass capillaries was observed at 270°C (**A**) and 500°C (**1**).

Keywords: crystal structure; decomposition behavior; germanium; pentamethylcyclopentadienyl; silicon; tin.

Introduction

The synthesis, characterization and functionalization of germanium-containing materials, which are, for example, suitable for energy transformation and storage, are currently investigated intensely (Wu et al., 2016). Molecular precursors are of interest as a result of their volatility and solubility, and examples such as GeH_2Ph_2, $GeH_2{}^tBu_2$, GeI_2 and GeH_3Cp^* were successfully employed to produce germanium nanowires (Lu et al., 2013; Mullane et al., 2013), nanoparticles (Zaitseva et al., 2007; Muthuswamy et al., 2013) and thin films (Dittmar et al., 2001; Dittmar, 2002), all of which hold great potential as anode materials for lithium ion batteries (Liang et al., 2013; Jin et al., 2014; Xiao and Cao, 2014; Xu et al., 2014; Sun et al., 2015). The germanes $GeH_2Cp_2^*$ (**1**) and $GeCl_2Cp_2^*$ (**A**) might serve as superior precursors as compared to the above mentioned examples, due to an expected combination of high volatility, low sensitivity towards air and moisture, long-term stability and low decomposition temperature. Synthesis protocols for $GeCl_2Cp_2^*$ (**A**) exist (Jutzi and Hielscher, 1985, 1986; Jutzi et al., 1986; Filippou et al., 2002), but $GeH_2Cp_2^*$ (**1**) was not reported so far. It is noteworthy that the syntheses for the lighter and the heavier homologues of **A**, $SiCl_2Cp_2^*$ (**B**) (Jutzi et al., 1986, 1988a,b, 1989; Evans et al., 1990) and $SnCl_2Cp_2^*$ (**C**) (Jutzi and Kohl, 1979; Jutzi et al., 1986; Naseri et al., 2010; Erickson et al., 2014), as well as for $SiH_2Cp_2^*$ (**D**) (Jutzi et al., 1988a,b; Dahlhaus et al., 1993) and $SiHClCp_2^*$ (**D**) (Jutzi et al., 1988a,1988b, 1993) are well documented, but only for the dichlorosilane **B** was the molecular structure in the solid state reported (Jutzi et al., 1988a,b). Herein, the synthesis and characterization of the germane $GeH_2Cp_2^*$ (**1**) is described, its thermal stability is compared with $GeCl_2Cp_2^*$ (**A**) and its molecular structure is discussed with comparison to other derivatives within the family of compounds of the type $MX_2Cp_2^*$ (M=Si, Ge, Sn; X=H, Cl).

Results and discussion

The organogermane **1** was synthesized by a hydrogenation reaction starting from $GeCl_2Cp^*_2$ (**A**) with $LiAlH_4$ in quantitative yield. It is worthy to note that various attempts to synthesize the heavier homologue $SnH_2Cp^*_2$ by hydrogenation of the stannane $SnCl_2Cp^*_2$ (**C**) with $LiAlH_4$ or diisobutylaluminum hydride (DIBAL-H) at either 20°C or −40°C failed, and an immediate reduction to elemental β-tin was always observed as indicated by powder X-ray diffraction (PXRD) analysis. The compounds of the type $MX_2Cp^*_2$ (**A**, M=Ge, X=Cl; **B**, M=Si, X=Cl; **C**, M=Sn, X=Cl; **D**, M=Si, X=H/Cl; **E**, M=Si, X=H) were prepared according

***Corresponding author: Michael Mehring,** Technische Universität Chemnitz, Fakultät für Naturwissenschaften, Institut für Chemie, Professur Koordinationschemie, D-09107 Chemnitz, Germany, e-mail: michael.mehring@chemie.tu-chemnitz.de
Ronny Fritzsche: Technische Universität Chemnitz, Fakultät für Naturwissenschaften, Institut für Chemie, Professur Koordinationschemie, D-09107 Chemnitz, Germany
Tobias Rüffer and Heinrich Lang: Technische Universität Chemnitz, Fakultät für Naturwissenschaften, Institut für Chemie, Professur Anorganische Chemie, D-09107 Chemnitz, Germany

to literature methods (Jutzi and Kohl, 1979; Jutzi et al., 1986, 1988a,b).

The ^{1}H NMR spectrum of **1** shows a singlet resonance corresponding to the GeH_2 protons at 3.91 ppm, which is shifted significantly downfield compared to the SiH_2 protons of $SiH_2Cp^*_2$ (**E**) (3.49 ppm) (Jutzi et al., 1988a,b), and the GeH_2 protons of other germanes, such as GeH_2Me_2 (3.72 ppm) (Erickson et al., 2014) or $GeH_2{}^tBu_2$ (3.67 ppm) (Kraft et al., 2011). The attenuated total reflectance Fourier transform infrared (ATR-FTIR) spectrum of **1** shows a strong band at 2008 cm^{-1} that is assigned to the Ge-H stretching vibration. Despite C_{2v} symmetry of **1**, only the $\nu_{sym}(GeH_2)$ vibration band is observed, which is in accordance with reports on other Cp substituted metal hydrides of C_{2v} symmetry such as MoH_2Cp_2 and WH_2Cp_2 (Girling et al., 1986; Belkova et al., 2012). This band is shifted to lower wavenumbers compared to its lighter homologue $SiH_2Cp^*_2$ (**E**) (2111 cm^{-1}). Similar to silane **E**, germane **1** is stable under inert conditions but decomposes slowly when it is exposed to air and moisture.

Single crystals of compounds **1** and **C–E** were grown by slow cooling of concentrated diethyl ether solutions containing the appropriate species to –30°C. The molecular structures of the germane **1**, stannane **C**, and silanes **D** and **E** are shown in Figures 1–4, and selected bond lengths (Å) and angles (°) are given in Table 1. The crystallographic parameters are summarized in Table 2.

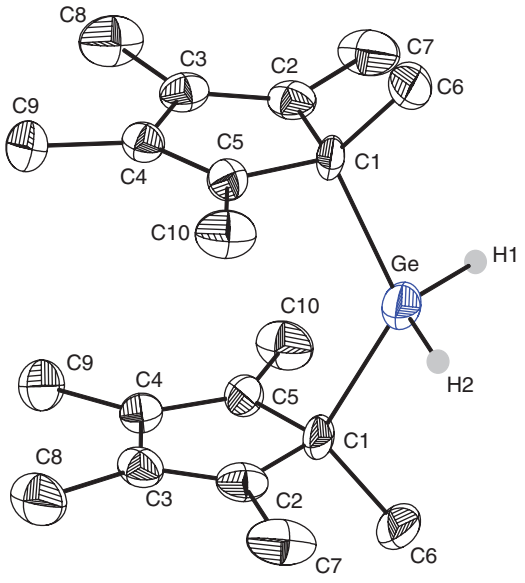

Figure 1: ORTEP at 40% probability for the carbon and germanium atoms and atom numbering scheme for compound **1**.
Hydrogen atoms of the methyl groups are omitted for clarity. Hydrogen atoms at the germanium are given in ball and stick type.

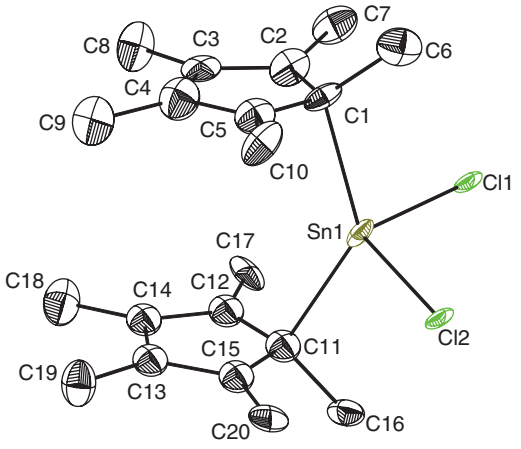

Figure 2: ORTEP at 50% probability and atom numbering scheme for compound **C**.
Hydrogen atoms of the methyl groups are omitted for clarity. Disorder of the chlorine atoms is not shown.

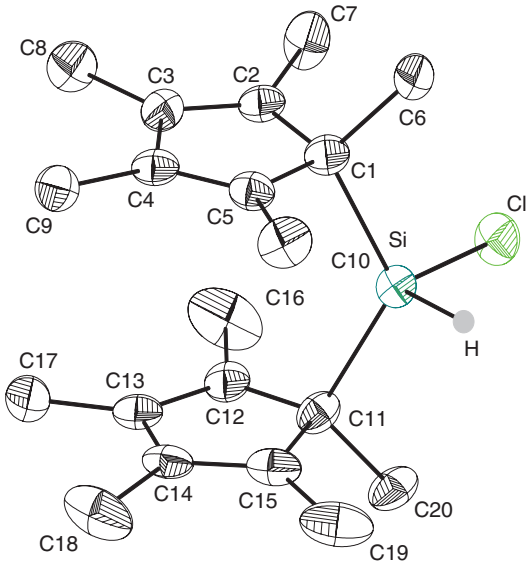

Figure 3: ORTEP at 20% probability and atom numbering scheme for compound **D**.
Hydrogen atom of the methyl groups are omitted for clarity. The hydrogen atom at the silicon is given in ball and stick type.

In all molecular structures of the type $MX_2Cp^*_2$ the metal atom (Si, Ge or Sn) is σ-bonded to the Cp* ring, and the latter exhibits a diene-like structure indicated by C-C single bonds (1.47–1.51 Å) and C=C double bonds (1.33–1.34 Å). The main features of all molecules are coplanar orientated Cp* rings, which are slightly parallel displaced and not congruent. This was also observed in the case of compounds such as SCp^*_2 (Bard et al., 1985), $BClCp^*_2$ (Macdonald et al., 2008), $PClCp^*_2$ (Pietschnig et al., 1997) and $(GaClCp^*_2)_2$ (Beachley et al., 1985). For germane **1** the Cp*

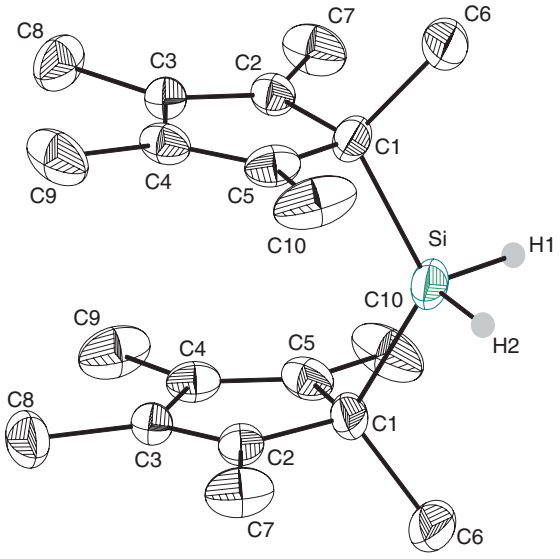

Figure 4: ORTEP at 40% probability and atom numbering scheme for compound **E**.
Hydrogen atoms of the methyl groups are omitted for clarity. Hydrogen atoms at the silicon are given in ball and stick type.

planes exhibit a dihedral angle (Table 1) of 5.43°, a value which is significantly lower than that of the corresponding silane **E** showing a value of 7.66°, but it is placed in the range as found for compounds **A–D** (5.15–5.83°). By contrast, the stannane **C** exhibits an angle of −6.90°, thus indicating attractive dispersion type interactions between the Cp* ligands. Compound **1** shows a typical parallel displacement of the Cp* groups (Table 1) of 19.10°, which is significantly larger than that in germane **B** with a value of 15.08°. A view along the *c* axis shows that the C1-M-C1′ plane (M=Si, Ge, Sn) (Table 1) is not orthogonal to the Cp* ring plane and is tilted by 5.56° for germane **1** and thus falls in the typical range from 3.89° to 6.83° (Table 1). As expected, the distance between the two Cp* ring centroids of 3.70 Å for **1** and 3.76 Å for **B** is greater, when compared to those of the silanes (3.52 Å), and less than for the tin homologues (3.92 Å). Due to the steric demand of the two Cp* rings, the tetrahedral angles around the germanium atom in compound **1** are significantly distorted C(1)*-Ge(1)-C(1) 121.4 (3)°, and the Ge-C bond is slightly elongated to 1.987 (4) Å as compared to GeH_2Mes_2 (1.965 Å) (Samanamu et al., 2011). The change of the metal atoms (Si, Ge and Sn) in the compounds **A–C** shows increasing M-C bond distances from 1.885 (3) (**B**), 1.977 (5) (**A**) to 2.172 (19) (**C**), leading to a decrease of intermolecular interaction between the two Cp* rings, and is reflected by the reduced Cp* dihedral angle and more parallel displacement.

The thermal behavior of the germane **1** and **A** was investigated by means of thermogravimetric analysis measurements and by temperature-dependent PXRD, with respect to our current interest in germanium-containing hybrid materials and thin films (Fritzsche and Mehring, 2016; Kitschke et al., 2016a,b). Heating to 550°C yielded a residue of 8.5% for **1** and 3.4% of **A** only, demonstrating significant volatility. The decomposition products from the thermogravimetric experiments were analyzed by energy dispersive X-ray/scanning electron

Table 1: Selected bond distances and angles of compounds **1** and **A–E**.

	$GeH_2Cp^*_2$ (1)	$GeCl_2Cp^*_2$ (A)	$SiCl_2Cp^*_2$ (B)	$SnCl_2Cp^*_2$ (C)	$SiHClCp^*_2$ (D)	$SiH_2Cp^*_2$ (E)
M	5.43°	5.90°	5.40°	−6.90°	5.15°	7.66°
	19.097 (2)°	15.1 (4)°	18.5 (2)°	19.182 (6)°	19.419 (6)°	18.892 (2)°
M	5.56°	3.90°	6.80 °	8.70°	4.77°	5.60°
M D	3.70 Å	3.80 Å	3.50 Å	3.92 Å	3.52 Å	3.57 Å
M-C	1.987 (4) Å	1.977 (5) Å	1.885 (3) Å	2.199 (2) Å	1.925 (15) Å	1.909 (2) Å
∠C-M-C	121.4 (3)°	127.3 (2)°	122.5 (1)°	129.733 (3)°	121.1 (7)°	121.3 (2)°
∠R-M-R (R=H; Cl)	123.632 (3)°	98.98 (11)°	101.08 (5)°	91.862 (4)°	110.246 (4)°	104.327 (2)°

Table 2: Crystallographic data of compounds **1**, **C**, **D** and **E**.

Compound	$GeH_2Cp^*_2$ (1)	$SnCl_2Cp^*_2$ (C)	$SiHClCp^*_2$ (D)	$SiH_2Cp^*_2$ (E)
Empirical formula	$GeC_{20}H_{32}$	$SnCl_2C_{20}H_{30}$	$SiClC_{20}H_{31}$	$SiC_{20}H_{32}$
Formula weight (g/mol)	345.04	460.03	334.99	300.54
Temperature (K)	105	120	180	105
Wavelength (Å)	1.54184	0.71073	1.54184	1.54184
Crystal system	Orthorhombic	Monoclinic	Monoclinic	Orthorhombic
space group	*Fdd*2	$P2_1$	*Cc*	*Fdd*2
a (Å)	29.8103 (16)	8.6158 (10)	8.6010 (18)	29.609 (2)
b (Å)	15.1892 (10)	15.4099 (14)	15.271 (2)	15.2187 (8)
c (Å)	8.4152 (6)	8.8565 (10)	15.7317 (2)	8.3873 (6)
α (°)	90	90	90	90
β (°)	90	116.660 (14)	104.98 (2)	90
γ (°)	90	90	90	90
V (Å^3)	3810.4 (4)	1050.9 (2)	1996.1 (5)	3779.5 (4)
Z	8	2	4	8
Density (calculated) (g/cm^3)	1.203	1.454	1.115	1.056
Absorption coefficient (mm^{-1})	2.101	1.468	2.210	1.014
F(000)	1472	468	728	1328
crystal size (mm^3)	0.4×0.3×0.2	0.4×0.4×0.14	0.16×0.16×0.14	0.24×0.22×0.12
θ range for data collection	5.94 to 62.99°	2.957 to 24.987	5.82 to 62.87°	5.98 to 62.71°
Limiting indices	$-34 \le h \le 30$	$-9 \le h \le 10$	$-9 \le h \le 8$	$-33 \le h \le 34$
	$-17 \le k \le 17$	$-18 \le k \le 18$	$-15 \le k \le 17$	$-17 \le k \le 17$
	$-9 \le l \le 9$	$-10 \le l \le 10$	$-12 \le l \le 18$	$-9 \le l \le 7$
Reflections collected	4464	9287	3112	5055
Independent reflections	1387 (R_{int} = 0.0298)	3663 (R_{int} = 0.0925)	1913 (R_{int} = 0.0409)	1270 (R_{int} = 0.0247)
Completeness	98.8%	99.7%	97.6%	99.2%
Refinement method	Full-matrix least-squares on F^2	Full-matrix least-squares on F^2	Full-matrix least-squares on F^2	Full-matrix least-squares on F^2
Data/restraints/parameters	1387/3/100	3663/228/169	1913/2/204	1270/2/100
Final *R* indices [$I > 2\sigma(I)$]	R_1 = 0.0534	R_1 = 0.0950	R_1 = 0.1302	R_1 = 0.0433
	wR_2 = 0.1387	wR_2 = 0.2283	wR_2 = 0.3325	wR_2 = 0.1256
R indices (all data)	R_1 = 0.0542	R_1 = 0.1013	R_1 = 0.1463	R_1 = 0.0438
	wR_2 = 0.1403	wR_2 = 0.2329	wR_2 = 0.3606	wR_2 = 0.1268
Goodness of fit on F^2	1.095	1.149	1.413	1.067
Largest difference peak and hole (eÅ^{-3})	1.095 and −0.375	1.348 and −1.555	0.747 and −0.437	0.207 and −0.172

microscope measurements, showing that the residue of germane **1** consists of 89.3% germanium, 9.4% carbon and 1.3% oxygen and the residue of germane **B** consists of 80.3% germanium, 17.6% carbon, 1.7% oxygen and 0.4% chlorine.

Temperature-dependent PXRD studies of $GeH_2Cp^*_2$ (**1**) measured in a sealed quartz glass capillary showed that reflections disappear at 85°C due to melting and crystalline germanium starts to form at around 550°C (Figure 5). The formation of germanium from $GeCl_2Cp^*_2$ (**B**) occurs at significantly lower temperatures than for germane **1** (Figure 6). The temperature-dependent PXRD analysis of **A** shows a phase transition at 140°C and the formation of crystalline germanium at 270°C. In the case of germane **1** the formation of amorphous germanium is assumed followed by crystallization between 500 and 600°C. It is noteworthy that the crystallization temperature of germanium depends significantly on the annealing conditions and preparation methods (Chik and Lim, 1976; Morimoto et al., 1984). The crystallization of amorphous germanium even below 400°C is reported if metals acting as nucleation seeds like Al [180°C (Toko et al., 2014) or 325°C (Oya et al., 2014)], Sn [450°C (Mullane et al., 2013)], Cu or Ag [380°C (Lu et al., 2013)] are present. The reason for the low crystallization temperature of **B** might be the presence of carbon. It has been reported that a phase segregation process from metastable germanium carbon alloys results in the formation of germanium nanocrystals even at low temperatures (Morimoto et al., 1984; John et al., 1997).

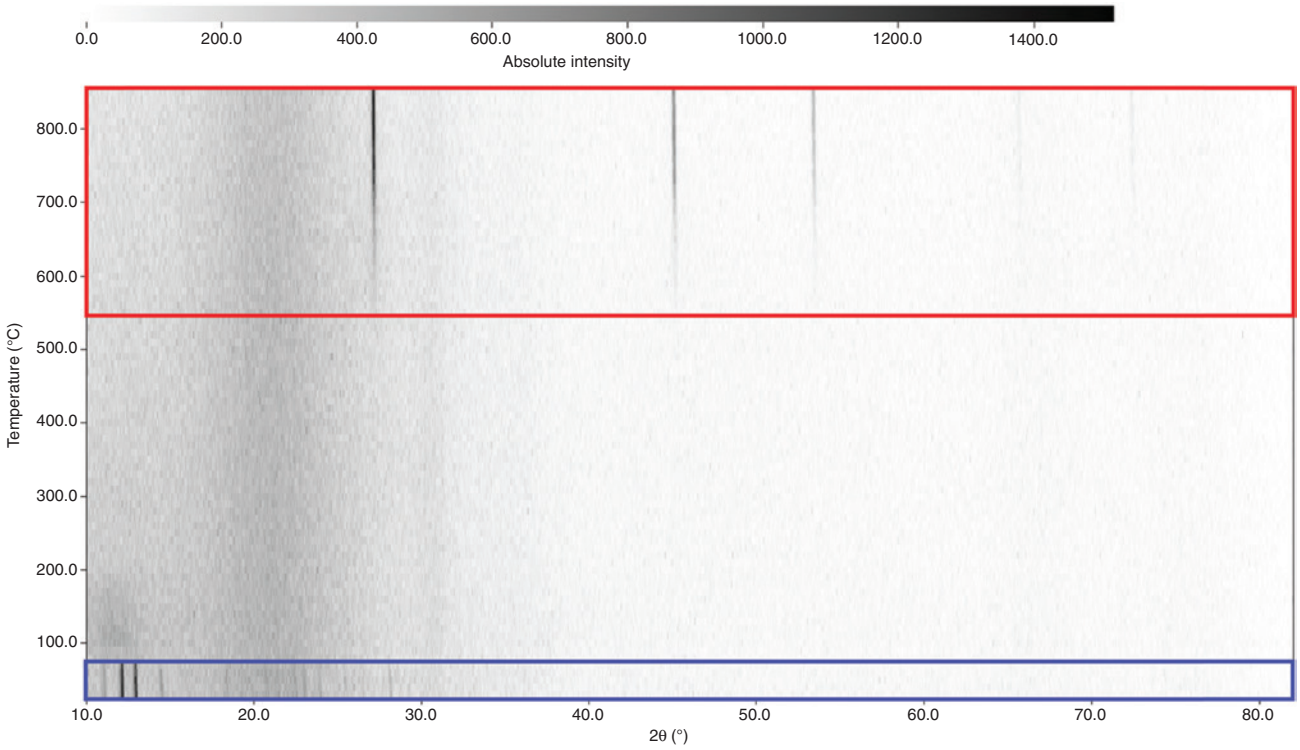

Figure 5: Temperature-dependent PXRD of **1** in sealed quartz glass capillaries confirming the formation of Ge (ICDD No. 00-004-0545).

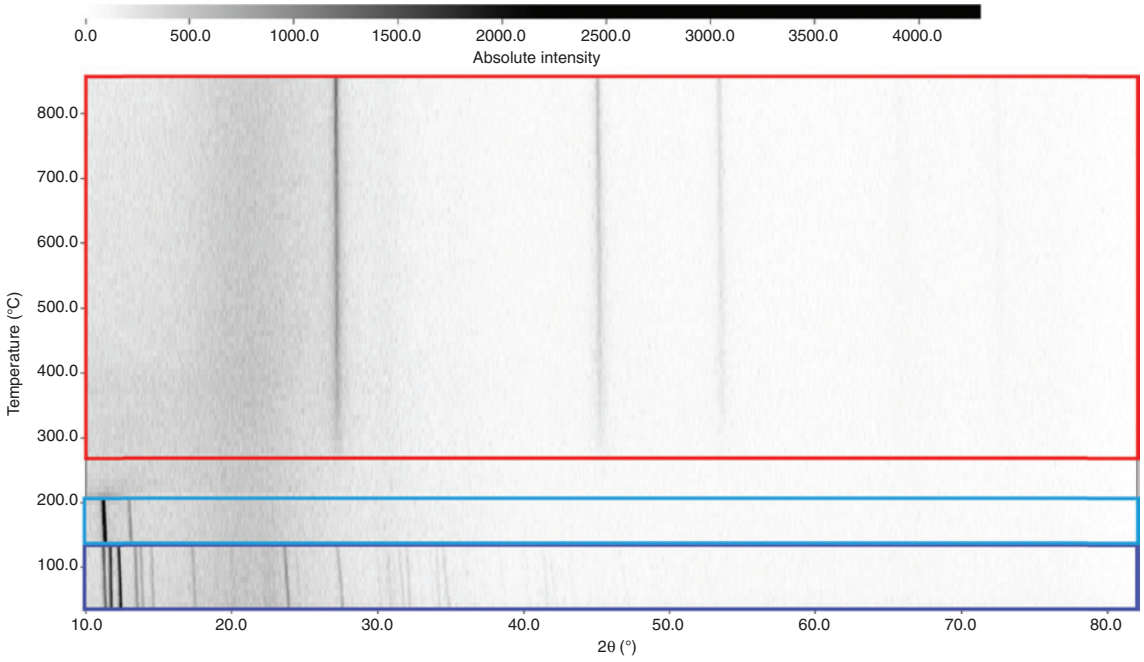

Figure 6: Temperature-dependent PXRD of **A** in sealed quartz glass capillaries, confirming the formation of Ge (ICDD No. 00-004-0545).

Conclusion

The germane $GeH_2Cp^*_2$ (**1**) was prepared in quantitative yield by hydrogenation of $GeCl_2Cp^*_2$ with $LiAlH_4$. Data obtained by ^1H and $^{13}C\{^1H\}$ NMR, ATR-FTIR spectroscopy and electron ionization (EI)-mass spectrometry (MS) are consistent with the formation of **1**. The molecular structure of **1** exhibits σ-bonded Cp* rings that are orientated parallel towards

each other, slightly parallel displaced and not congruent. Similar structures are observed for compounds of the type $MX_2Cp^*_2$ (**C**, M=Sn, X=Cl; **D**, M=Si, X=H/Cl; **E**, M=Si, X=H). All compounds, despite $SnCl_2Cp^*_2$ (**C**), show Cp* rings, that are tilted against each other. Thermal analysis is consistent with the formation of crystalline germanium upon decomposition. Thus, the volatile germane **1** might be used for deposition of germanium thin films at rather low temperature.

Experimental section

General procedure

All reactions were carried out under argon atmosphere using standard Schlenk techniques or in a glovebox under argon atmosphere. Diethyl ether, tetrahydrofuran, toluene and *n*-hexane were purified by distillation from sodium. CH_3CN was dried prior to use by distillation from CaH_2. All other chemicals were purchased from commercial suppliers. *n*-Butyl lithium (2.5 M in *n*-hexane, Acros Organics, Hampton, NH, USA), lithium aluminum hydride (97%, Alfa Aesar, Ward Hill, MA, USA), $SiCl_4$ (99%, Alfa Aesar, Ward Hill, MA, USA), $SiHCl_3$ (99%, Sigma-Aldrich, St. Louis, MO, USA), $GeCl_4$ (99%, ABCR, Karlsruhe, Germany), $SnCl_4$ (99%, Sigma-Aldrich, St. Louis, MO, USA) and DIBAL-H (97%, Sigma-Aldrich, St. Louis, MO, USA) were used as received. 1,2,3,4,5-Pentamethylcyclopentadiene (Cp*H) (Fendrick et al., 1992), **A** (Jutzi et al., 1986), **B** (Jutzi et al., 1988a,b), **C** (Jutzi et al., 1986), **D** (Jutzi et al., 1988a,b) and **E** (Jutzi et al., 1988a,b) were synthesized according to literature methods. The lithium salt of Cp* was synthesized according to modified literature procedures with *n*-butyllithium in tetrahydrofuran (Jutzi et al., 1988a,b).

ATR-FTIR spectra were measured with a BioRad FT-IR 165 spectrometer (Bio-Rad Laboratories, Philadelphia, PA, USA) with Golden Gate ATR (LOT-Oriel GmbH and Co. KG, Darmstadt, Germany). NMR spectra were recorded using a Bruker Avance III 500 (Bruker Corporation, Billerica, MA, USA) (500.3 MHz for ^1H, 125.7 MHz for $^{13}C\{^1H\}$). Chemical shifts (δ) are reported in parts per million (ppm) relative to tetramethylsilane (TMS) using the solvent as internal reference ($CDCl_3$: ^1H NMR δ 7.26 ppm). Microanalysis was performed by using a Thermo Fischer FlashAE 1112 (Thermo Fisher Scientific Inc., Waltham, MA, USA). The melting points (sealed off in argon flushed capillaries) were determined using a Büchi Melting Point B-540 (Büchi Labortechnik GmbH, Essen, Germany). EI-MS was performed with a Shimadzu GC-17A Gas Chromatograph and GC-MS-QP5000 Gas Chromatograph Mass Spectrometer (Shimadzu Corp, Kyōto, Japan). The PXRD patterns were collected using a STOE-STAD IP diffractometer from STOE (STOE and Cie GmbH, Darmstadt, Germany) with Cu-K_α radiation (40 kV, 40 mA) and a Ge (111) monochromator. All decomposition experiments were carried out in a nitrogen filled glovebox (M. Braun Inertgas-Systeme GmbH, Garchingen, Germany) in silver cups on a ceramic heater up to 550°C.

Crystallographic studies

All data were collected on an Oxford Gemini S diffractometer (Agilent Technologies Sales and Services GmbH and Co. KG, Life Sciences and Chemical Analysis, Waldbronn, Germany) using graphite-monochromatized Cu-K_α radiation ($\lambda = 1.54184$ Å). The structures of **1**, **C**, **D** and **E** were solved by direct methods using SHELXS-2013 and refined by full-matrix least-squares procedures on F^2 using SHELXL-2013 (Sheldrick 2013). All non-hydrogen atoms were refined anisotropically. All C-bonded hydrogen atoms were geometrically placed and refined isotropically in riding modes using appropriate SHELXL-2013 HFIX constraints. The positions of Si- and Ge-bonded hydrogen atoms were taken from difference Fourier maps and refined isotropically. Data have been deposited at the Cambridge Crystallographic Data Centre under the CCDC deposition numbers 1526800 (**1**), 1526803 (**C**), 1526801 (**D**) and 1526802 (**E**).

Due to a phase transition below approximately 160 K the single crystal of **D** had been measured at 180 K. Due to higher measurement temperature, U_{ij} values especially of the carbon atoms of the Cp* ligands are comparatively large. Trials to refine each of the two independent disordered Cp* rings on two positions failed. Nevertheless, valid results for compound **D** were obtained. Crystallographic data for **A** and **B** were extracted from the cif-files [No. 180860 (**A**) and No. 1166703 (**B**)] deposited at the CCDC.

Synthesis of $GeH_2Cp^*_2$ (1)

Lithium aluminum hydride (0.10 g, 24 mmol) was added in a single portion to a solution of $GeCl_2Cp^*_2$ (**A**) (1.00 g, 2.4 mmol) in tetrahydrofuran (30 mL) at −80°C. The grey suspension was stirred for 1.5 h at 20°C, and then the solvent was removed under reduced pressure and *n*-hexane (30 mL) was added. The suspension was then filtered through celite, and evaporation of *n*-hexane in vacuum gave a colorless solid. Single crystals suitable for X-ray analysis were grown from a CH_3CN solution at −30°C.

Yield: 0.81 g (98%) colorless solid, with mp. 83–85°C, decomposition 200°C. Elemental analysis (%) calcd. for $C_{18}H_{32}Ge$ (345.11): C, 69.61; H, 9.35; Found: C, 69.34; H, 9.73. EI-MS: *m/z* 346 $[M]^+$ (1.4%), *m/z* 209 $[C_{10}H_{15}Ge]^+$ (100%). ATR-FTIR [cm^{-1}]: ν(CH_3) 2913 (s), 2857 (s), ν(Ge-H) 2008 (s), 870 (s), 743 (s), 724 (s). ^1H NMR (500 MHz, $CDCl_3$): δ 1.70 [s br, 30H $C_5(CH_3)_5$], 3.91 [s, 2H, GeH_2]. ^{13}CNMR (125 MHz, $CDCl_3$): δ 10.33 [s, $C_5(CH_3)_5$], 135.25 [s, $C_5(CH_3)_5$].

Acknowledgements: We gratefully acknowledge the BMBF (Project No. 214648), the SMWK (Project No. 4-7531.50/1128/1) and the Fonds der Chemischen Industrie for financial support.

References

Bard, A. J.; Cowley, A. H.; Leland, J. K.; Thomas, G. J. N.; Norman, N. C.; Jutzi, P.; Morley, C. P.; Schlüter, E. Synthesis, structures, and reactivities of some pentamethylcyclopentadienyl-sulphur compounds. *Dalton Trans.* **1985**, 1303–1307.

Beachley, O. T.; Hallock, R. B.; Zhang, H. M.; Atwood, J. L. Syntheses, characterizations, and crystal and molecular structures of (pentamethylcyclopentadienyl)gallium chlorine compounds $Ga(C_5Me_5)_2Cl$ and $Ga(C_5Me_5)Cl_2$. *Organometallics* **1985**, *4*, 1675–1680.

Belkova, N. V.; Epstein, L. M.; Filippov, O. A.; Shubina, E. S. Spectroscopic Properties of Inorganic and Organometallic Compounds: Techniques, Materials and Applications, Vol. 43, The Royal Society of Chemistry: London, UK, 2012, pp. 1–28.

Chik, K. P.; Lim, P.-K. Annealing and crystallization of amorphous germanium thin films. *Thin Solid Films* **1976**, *35*, 45–56.

Dahlhaus, J.; Jutzi, P.; Frenck, H. J.; Kulisch, W. Pentamethylcyclopentadienyl-substituted silanes $(Me_5C_5)SiH_3$ and $(Me_5C_5)_2SiH_2$ as precursors for low-temperature remote plasma-enhanced CVD of thin silicon nitride and silica films. *Adv. Mater. (Weinheim, Fed. Repub. Ger.)* **1993**, *5*, 377–380.

Dittmar, K. PhD thesis, University Bielefeld **2002**.

Dittmar, K.; Jutzi, P.; Schmalhorst, J.; Reiss, G. Cyclopentadienyl germanes as novel precursors for the CVD of thin germanium films. *Chem. Vap. Deposition* **2001**, *7*, 193–195.

Erickson, K. A.; Dixon, L. S. H.; Wright, D. S.; Waterman, R. Exploration of tin-catalyzed phosphine dehydrocoupling: catalyst effects and observation of tin-catalyzed hydrophosphination. *Inorg. Chim. Acta* **2014**, *422*, 141–145.

Evans, W. J.; Ulibarri, T. A.; Jutzi, P. Relative reactivity of decamethylsilicocene and decamethylsamarocene: reduction of $(C_5Me_5)_2SiCl_2$ by samarium(II) reagents. *Inorg. Chim. Acta* **1990**, *168*, 5–6.

Fendrick, C. M.; Schertz, L. D.; Mintz, E. A.; Marks, T. J.; Bitterwolf, T. E.; Horine, P. A.; Hubler, T. L.; Sheldon, J. A.; Belin, D. D. Large-scale synthesis of 1,2,3,4,5-pentamethylcyclopentadiene. *Inorg. Synth.* **1992**, *29*, 193–198.

Filippou, A. C.; Portius, P.; Philippopoulos, A. I. Molybdenum and tungsten germylyne complexes of the general formula trans-$[X(dppe)_2Mo{\equiv}Ge\text{-}(\eta^1\text{-}Cp)]$ (X = Cl, Br, I; dppe = $Ph_2PCH_2CH_2PPh_2$; Cp = C_5Me_5): syntheses, molecular structures, and bonding features of the germylyne ligand. *Organometallics* **2002**, *21*, 653–661.

Fritzsche, R.; Mehring, M. Deposition of thin germanium films on flexible substrates. *Z. Anorg. Allg. Chem.* **2016**, *642*, 1047.

Girling, R. B.; Grebenik, P.; Perutz, R. N. Vibrational spectra of terminal metal hydrides: solution and matrix-isolation studies of $[(m\text{-}C_5H_5)_2MH_n]^{x+}$ (M = Re, Mo, W, Nb, Ta; n = 1–3; x = 0, 1). *Inorg. Chem.* **1986**, *25*, 31–36.

Jin, S.; Li, N.; Cui, H.; Wang, C. Embedded into graphene Ge nanoparticles highly dispersed on vertically aligned graphene with excellent electrochemical performance for lithium storage. *ACS Appl. Mater. Interfaces* **2014**, *6*, 19397–19404.

John, T.-M.; Veit, P.; Anton, R.; Drüsedau, T. P. Germanium-carbon multilayer films prepared by magnetron sputtering – structure and thermally induced formation of Ge-nanocrystals. *Thin Solid Films* **1997**, *296*, 69–71.

Jutzi, P.; Kohl, F. Synthesis and reactions of pentamethylcyclopentadienyltin compounds. *J. Organomet. Chem.* **1979**, *164*, 141–152.

Jutzi, P.; Hielscher, B. A new approach to Group IVB metallocenes. *J. Organomet. Chem.* **1985**, *291*, C25–C27.

Jutzi, P.; Hielscher, B. Preparation of tin and germanium metallocenes from tetravalent precursors. *Organometallics* **1986**, *5*, 1201–1204.

Jutzi, P.; Kanne, D.; Krüger, C. Decamethylsilicocene – synthesis and structure. *Angew. Chem.* **1986**, *98*, 163–164.

Jutzi, P.; Holtmann, U.; Bogge, H.; Müller, A. Protonation of decamethylsilicocene [bis(pentamethylcyclopentadienyl)silicon]. *J. Chem. Soc., Chem. Commun.* **1988a**, 305–306.

Jutzi, P.; Kanne, D.; Hursthouse, M.; Howes, A. J. Mono- and bis(η^1-pentamethylcyclopentadienyl)silanes. Synthesis, structure, and properties. *Chem. Ber.* **1988b**, *121*, 1299–1305.

Jutzi, P.; Holtmann, U.; Kanne, D.; Krüger, C.; Blom, R.; Gleiter, R.; Hyla-Kryspin, I. Decamethylsilicocene – the first stable silicon(II) compound: synthesis, structure, and bonding. *Chem. Ber.* **1989**, *122*, 1629–1639.

Jutzi, P.; Bunte, E.-A.; Holtmann, U.; Neumann, B.; Stammler, H.-G. Chemistry of decamethylsilicocene: oxidative addition of compounds with X-H bonds (X = F, Cl, Br, O, S). *J. Organomet. Chem.* **1993**, *446*, 139–147.

Kitschke, P.; Walter, M.; Rüffer, T.; Lang, H.; Kovalenko, M. V.; Mehring, M. From molecular germanates to microporous Ge@C via twin polymerization. *Dalton Trans.* **2016a**, *45*, 5741–5751.

Kitschke, P.; Walter, M.; Rüffer, T.; Seifert, A.; Speck, F.; Seyller, T.; Spange, S.; Lang, H.; Auer, A. A.; Kovalenko, M. V., et al. Porous Ge@C materials via twin polymerization of germanium(ii) salicyl alcoholates for Li-ion batteries. *J. Mater. Chem. A* **2016b**, *4*, 2705–2719.

Kraft, A.; Beck, J.; Krossing, I. Facile access to the pnictocenium ions $[Cp^*ECl]^+$ (E = P, As) and $[(Cp^*)_2P]^+$: chloride ion affinity of $Al(OR^F)_3$. *Chem. - Eur. J.* **2011**, *17*, 12975–12980.

Liang, W.; Yang, H.; Fan, F.; Liu, Y.; Liu, X. H.; Huang, J. Y.; Zhu, T.; Zhang, S. Tough germanium nanoparticles under electrochemical cycling. *ACS Nano* **2013**, *7*, 3427–3433.

Lu, X.; Harris, J. T.; Villarreal, J. E.; Chockla, A. M.; Korgel, B. A. Enhanced nickel-seeded synthesis of germanium nanowires. *Chem. Mater.* **2013**, *25*, 2172–2177.

Macdonald, C. L. B.; Gorden, J. D.; Voigt, A.; Filipponi, S.; Cowley, A. H. Group 13 decamethylmetallocenium cations. *Dalton Trans.* **2008**, 1161–1176.

Morimoto, A.; Kataoka, T.; Kumeda, M.; Shimizu, T. Annealing and crystallization processes in tetrahedrally bonded binary amorphous semiconductors. *Philos. Mag. B* **1984**, *50*, 517–537.

Mullane, E.; Kennedy, T.; Geaney, H.; Dickinson, C.; Ryan, K. M. Synthesis of tin catalyzed silicon and germanium nanowires in a solvent-vapor system and optimization of the seed/nanowire interface for dual lithium cycling. *Chem. Mater.* **2013**, *25*, 1816–1822.

Muthuswamy, E.; Iskandar, A. S.; Amador, M. M.; Kauzlarich, S. M. Facile synthesis of germanium nanoparticles with size control: microwave versus conventional heating. *Chem. Mater.* **2013**, *25*, 1416–1422.

Naseri, V.; Less, R. J.; Mulvey, R. E.; McPartlin, M.; Wright, D. S. Stoichiometric and catalytic Sn-mediated dehydrocoupling of primary phosphines. *Chem. Commun.* **2010**, *46*, 5000–5002.

Oya, N.; Toko, K.; Saitoh, N.; Yoshizawa, N.; Suemasu, T. Direct synthesis of highly textured Ge on flexible polyimide films by metal-induced crystallization. *Appl. Phys. Lett.* **2014**, *104*, 262107.

Pietschnig, R.; Ebels, J.; Nieger, M.; Zoche, N.; Jansen, M.; Niecke, E. Synthetic Approach and Structural Comparison of Some Novel Phosphanes of the Type $(C_5Me_5)_2PX$ (X = F, Cl, Br, I), Vol. 134, Elsevier Science: Amsterdam, Netherlands, **1997**.

Samanamu, C. R.; Anderson, C. R.; Golen, J. A.; Moore, C. E.; Rheingold, A. L.; Weinert, C. S. Syntheses and structural analysis of the sterically encumbered germanes $(o\text{-}But C_6H_4)_3GeX$ (X = Br, H, Cl, OH), $(o\text{-}But C_6H_4)_2GeBr_2$, and Mes_2GeH_2: distortions arising from the presence of an *ortho-tert*-butyl substituent. *J. Organomet. Chem.* **2011**, *696*, 2993–2999.

Sheldrick, G. M. *SHELXS-/SHELXL-2013, University of Göttingen, Program for Crystal Structure Solution/Refinement* **2013**.

Sun, Y.; Jin, S.; Yang, G.; Wang, J.; Wang, C. Germanium nanowires-in-graphite tubes via self-catalyzed synergetic confined growth and shell-splitting enhanced Li-storage performance. *ACS Nano* **2015**, *9*, 3479–3490.

Toko, K.; Numata, R.; Oya, N.; Fukata, N.; Usami, N.; Suemasu, T. Low-temperature (180 °C) formation of large-grained Ge (111) thin film on insulator using accelerated metal-induced crystallization. *Appl. Phys. Lett.* **2014**, *104*, 022106.

Wu, S.; Han, C.; Iocozzia, J.; Lu, M.; Ge, R.; Xu, R.; Lin, Z. Germanium-based nanomaterials for rechargeable batteries. *Angew. Chem., Int. Ed.* **2016**, *55*, 7898–7922.

Xiao, Y.; Cao, M. High-performance lithium storage achieved by chemically binding germanium nanoparticles with N-doped carbon. *ACS Appl. Mater. Interfaces* **2014**, *6*, 12922–12930.

Xu, Y.; Zhu, X.; Zhou, X.; Liu, X.; Liu, Y.; Dai, Z.; Bao, J. Ge nanoparticles encapsulated in nitrogen-doped reduced graphene oxide as an advanced anode material for lithium-ion batteries. *J. Phys. Chem. C* **2014**, *118*, 28502–28508.

Zaitseva, N.; Dai, Z. R.; Grant, C. D.; Harper, J.; Saw, C. Germanium nanocrystals synthesized in high-boiling-point organic solvents. *Chem. Mater.* **2007**, *19*, 5174–5178.